International Journal of Nanomedicine

Dovepress
open access to scientific and medical research

Open Access Full Text Article

ORIGINAL RESEARCH

Wound-healing effect of micronized sacchachitin (*m*SC) nanogel on corneal epithelium

This article was published in the following Dove Press journal:
International Journal of Nanomedicine
27 August 2012
Number of times this article has been viewed

Ray-Neng Chen[1,*]
Lin-Wen Lee[2,5,*]
Ling-Chun Chen[3]
Hsiu-O Ho[3]
Shiao-Chuan Lui[2]
Ming-Thau Sheu[3,4]
Ching-Hua Su[2]

[1]Department of Cosmetic Science and Management, Mackay Medicine, Nursing and Management College, Taipei, [2]Department of Microbiology and Immunology, School of Medicine, College of Medicine, [3]School of Pharmacy, College of Pharmacy, [4]Clinical Research Center and Traditional Herbal Medicine Research Center, Taipei Medical University Hospital, Taipei Medical University, [5]Research Center for Biomedical Devices and Prototyping Production, Taipei Medical University, Taipei, Taiwan, Republic of China

*These authors contributed equally to this work

Abstract: The extraction residue of the *Ganoderma* fruiting body, named sacchachitin, has been demonstrated to have the potential to enhance cutaneous wound healing by inducing cell proliferation. In this study, a nanogel formed from micronized sacchachitin (*m*SC) was investigated for the potential treatment of superficial chemical corneal burns. Reportedly, *m*SC has been produced successfully and its chemical properties confirmed, and physical and rheological properties characterized. An in vitro cell proliferation study has revealed that at the concentrations of 200, 300, and 400 μg/mL, *m*SC nanogel significantly increased Statens Seruminstitut rabbit corneal (SIRC) cell proliferation after 24 hours of incubation. In cell migration assay, migration of SIRC cell to wound closure was observed after 24 hours of incubation with the addition of 200 μg/mL *m*SC of nanogel. In an animal study, acceleration of corneal wound healing was probably due to the inhibition of proteolysis. In conclusion, the findings of this study substantiate the potential application of sacchachitin in the form of *m*SC nanogel for the treatment of superficial corneal injuries.

Keywords: corneal wound healing, sacchachitin, matrix metalloproteinase

Introduction

Ocular burns are classified based on their etiologies as radiant energy injuries (either thermal or ultraviolet) or chemical exposures (acid or alkali), with the latter tending to carry a worse prognosis compared with the former. Potential management strategies of ocular thermal and chemical injuries have been proposed.[1,2] In brief, once patients suffering from a chemical injury present to the emergency department of a hospital, the chemical should be identified if possible but treatment of the patient should not be delayed. Immediate treatment should include copious irrigation to neutralize the pH prior to ophthalmic injury evaluation. Once the pH has been neutralized and the patient has been more thoroughly examined, then attention must be directed toward treating the injuries the patient has received. This treatment consists mainly of promoting the healing of the corneal epithelium and treating the intraocular pressure if elevated. If the extent of the injury is minor, preservative-free artificial tears are usually adequate to promote re-epithelization. If there is extensive damage and necrosis, the patient may be well served by undergoing debridement of the necrotic tissue. Following debridement, there may be a potential role for amniotic membrane grafting to enhance epithelial regeneration while suppressing perilimbal inflammation. Amniotic membrane transplantation (AMT) assists in the restoration of the conjunctival surface and reduction of limbal stromal inflammation and can be applied in both the acute and chronic setting following a chemical or thermal injury.[3–5]

Correspondence: Ching-Hua Su; Ming-Thau Sheu
250 Wu-Hsing Street, Taipei, Taiwan 110, Republic of China
Tel +886 2 2377 1942
Email curator@tmu.edu.tw; mingsheu@tmu.edu.tw

submit your manuscript | www.dovepress.com
Dovepress
http://dx.doi.org/10.2147/IJN.S34530

Overall, following a chemical or thermal injury, corneal re-epithelization with preservative-free artificial tears for minor injuries or amniotic membrane grafting to promote epithelial regeneration for extensive damage of corneal areas helps to heal corneal wounds. Corneal wound healing is a dynamic process involving a coordinated cascade of cytokine-mediated interactions between the epithelial cells, stromal keratocytes, and cells of the immune system. The healing process of a corneal epithelial wound can be categorized in three different phases: (1) latent phase; throughout this phase, polymorphonuclear leukocytes deal with the removal of necrotic cells with the rounding and retraction of epithelial cells observed at the wound edge; (2) cell migration and adhesion phase; an epithelial monolayer covers the wound area and epithelial restoration and stromal adhesion are seen; (3) cell proliferation phase; proliferation of the epithelial cells until normal epithelial thickness is restored. The healing process is influenced by many factors including the size and depth of the wound, causative agent, and tear quality.[6–8]

In a few cases of corneal tissue damage, a close balance between stromal extracellular matrix (ECM) reconstruction and degradation is disrupted, resulting in a chronic wound-healing condition. There is a large amount of evidence regarding matrix metalloproteinases (MMPs), which play a key factor in the regulation of inflammation, degrading, and remodeling of the new ECM during the wound-healing process. As part of the tissue response to injury, the activity of MMP is strictly regulated at various levels including gene expression and the tissue inhibitors of MMPs (TIMPs). All classes of extracellular matrix proteins and signaling molecules such as cytokines and growth factors are substrates for the MMPs.[9–11] Gelatinases, in this case MMP-2 and MMP-9, play a significant role in the remodeling of the corneal stromal ECM and the reformation of the epithelial basement membrane.[12,13] MMP-9, also known as gelatinase B, is secreted by corneal epithelial cells, macrophages, and neutrophils during corneal wound healing. The changes in level of MMPs in the tear film and expression of MMP in the cornea during wound healing have been described. Higher levels of MMP-9 are found in the corneal epithelium of those patients with pseudophakic corneal edema.[14–16]

Many attempts have previously been made to promote corneal wound repair. In the 1940s, rabbit peritoneum was used to cover the acutely burned ocular surface, which successfully promoted healing and prevented the spread of necrosis to adjacent tissues. The use of amniotic membrane for the treatment of various corneal injuries and ocular surface diseases has been explored following the results of experiments. Varying clinical success rates have resulted due to the limited availability of the amniotic membrane, risks of transmissible infections, and biological composition of membranes.[17–19] To avoid the complications of using amniotic membrane, alternative regimens including various drug systems such as collagen shields, eye drops, autologous platelet concentrate, regenerative factor-rich plasma, ointments, and polymeric hydrogels as a drug reservoir have been widely investigated.[20–25] A biodegradable, amphiphilic triblock copolymer, for example, poly(DL-lactide-co-glycolide-b–ethylene glycol-b-DL-lactide-co-glycolide) (PLGA–PEG–PLGA), was proven to be a potential bandage by its gelling profile and biocompatibility properties.[26] Anumolu and colleagues demonstrated that poly(ethyleneglycol) (PEG)-based doxycycline hydrogel accelerated corneal wound healing in half-mustard and nitrogen mustard-exposed rabbit corneas in organ culture.[27] Further, the application of these materials obtained from nature to promote corneal injury was also evaluated. Membrane combining chitosan and poly-D,L-lactic acid indicated the potential for treating alkali-burned rabbit cornea.[28]

The medicinal fungus, *Ganoderma tsugae*, also commonly known as Hemlock varnish shelf mushroom or tree mushroom, has been used as a traditional medicine since ancient times in Asian countries. In our previous research, the extraction residue of the *Ganoderma* fruiting body, named sacchachitin, demonstrated the potential of enhancing cutaneous wound healing by inducing cell proliferation.[29–31] Nanogel was formed when fibrous sacchachitin was micronized and dispersed in aqueous medium. In the present study, nanogel formed from micronized sacchachitin (*m*SC) was investigated for the potential treatment of superficial chemical corneal burns. The possible mechanism of enhancing corneal wound repair was also examined by determining MMP-9 activity and cell migration assay.

Materials and methods

Materials

Statens Seruminstitut rabbit cornea (SIRC) cells were purchased from Bio-resource Collection and Research Center (Hsinchu, Taiwan). Zoletil (virbac) was supplied by Sigma Co (St Louis, MO). N-acetyl-glucosamine, chitin, chitosan, p-dimethylaminobenzaldehyde, 3,5-dinitrosalicylic acid, dipotassium tetraborate tetrahydrate, gelatin, glucosamine, potassium phosphate monobasic (KH_2PO_4), silica gel, and sodium phosphate dibasic ($Na_2HPO_4 \cdot 7H_2O$) were obtained from Merck Co (Darmstadt, Germany).

Preparation of micronized sacchachitin (*m*SC) nanogel

Sacchachitin was prepared from the residue of the fruiting body of *Ganoderma tsugae*, which was obtained by solid state cultivation. The method of preparation follows as reported in the previous paper.[30] In brief, 1,000 grams of the residue were pulverized and extracted with ethanol for 48 h. The residue was collected and blow-dried at 40°C. The dried mixture was then digested with 1N NaOH at 85°C for 24 h. The residue was collected and washed with deionized water to remove any residual $NaOH \cdot H_2O_2$ (1:3 to weight of the residue) was then used for pigmentation. After removal of any residual H_2O_2 by repeated washing with deionized water, the pulp-like residue was further sieved to obtain fibers with the length of 10–50 μm. Sacchachitin so obtained was micronized into fine powder by the bead-milling method using NANO-M2 model (ITRI; Hsinchu, Taiwan) with specifications of grinding media, ϕ 0.1 mm YTZ; pin type; rotor speed, 18 m/s. *m*SC nanogel (Figure 1) was prepared by adding *m*SC micronized powder to the sterilized phosphate-buffered saline (PBS) before application in the study. *m*SC was characterized using size-exclusion chromatography and thin-layer chromatography as described previously.

Physical analysis and rheological measurement of *m*SC

The length of *m*SC fibers expressed as effective diameter was measured at room temperature using a Brookhaven 90Plus Particle Size Analyzer (Brookhaven Instruments Corp, Holtsville, NY). Each sample was measured in duplicate. Zeta potential was measured in purified water using the same equipment. HAAKE RheoStress 1 (Thermo Fisher Scientific Inc, Rockford, IL) equipped with a Cone Ø60 mm, 1° angle (C60/1) was used to measure the rheological properties of the nanogel aqueous dispersions. Steady rate sweep test of nanogel aqueous dispersions was carried out at 25°C to measure steady viscosity (η) as a function of shear rates from 0.1 to 500 s^{-1}. To establish the linear viscoelastic region, the rheological parameters, elastic modulus G′ (storage modulus), viscous modulus G″ (loss modulus), and complex viscosity (η*) were measured as functions of stress (τ, 0.2–20 Pa) at an angular frequency of 1 Hz at 25°C. Once the linear viscoelastic region was established, subsequent measurements were conducted at a fixed stress (τ = 1.0 and 1.5 Pa) within the linear viscoelastic region. A dynamic frequency sweep was carried out at 25°C to record the viscoelastic parameters changing in frequency from 0.1 to 100 Hz. The changing of the rheological parameters with temperature were measured at a fixed frequency of 1 Hz and a fixed stress (1.0 Pa) in the temperature range of 15°C –60°C at a heating rate of 1.5°C/min.

MTT cell proliferation study

The effect of *m*SC nanogel on SIRC cell proliferation was examined by 3-(4,5-dimethylthiazol-2-yl)-2,5-diphenyltetrazolium bromide (MTT) assay. SIRC cells at a concentration of 1×10^4 cells/well were seeded on 24-well plates and

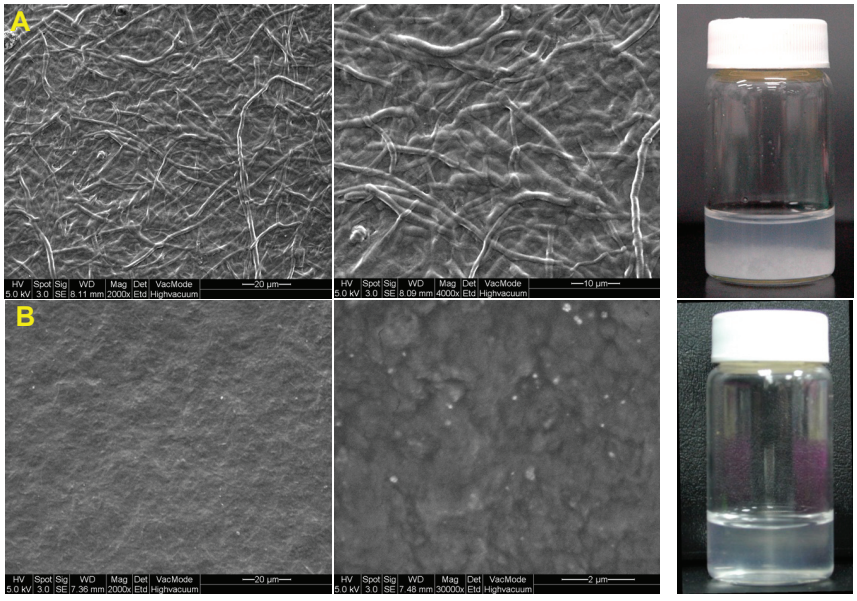

Figure 1 Micronized sacchachitin suspension (200 μg/mL) and scanning electron microscopy photographs for fibrous (**A**) and micronized sacchachitin (**B**).

incubated using MEM with 10% (v/v) fetal bovine serum as the medium. After incubating for 24 h, the medium was changed for a fresh medium containing various concentrations of *m*SC nanogel (50, 100, 200, 300, 400, and 500 μg/mL) and the incubation was further continued for 24 and 48 h, respectively. After the culture was done for the indicated periods, 50 μL of MTT was added to each well and was again incubated for an additional 4 h at 37°C. The supernatant was removed and 120 μL of DMSO was added to each of the wells in order to dissolve the water-insoluble purple formazan crystals, which were then transferred to 96-well microplates for reading. The absorbing rate was measured using a multi-well spectrophotometer (Titertek Multiscan; Flow Labs, Irvine, UK) at a wavelength of 550 nm. MTT cell proliferation studies were performed in triplicate (three separate experiments).

Cell migration assay

SIRC cells were incubated using MEM with 10% (v/v) fetal bovine serum as the medium in a Petri dish 35 mm in diameter until the growth fully covered the whole dish. A cell lifter was used to scratch a line across the center of the dish. The remaining cells on both sides were washed twice with PBS. Then, a medium (MEM with 10% [v/v] fetal bovine serum) containing 200 μg/mL of *m*SC nanogel was added and incubated for 24 h at 37°C with 5% CO_2. Simultaneously, a control study was done using the medium without *m*SC nanogel. The extent of migration was photographed and estimated with three separate experiments (triplicate).

Animal studies

Female New Zealand white rabbits weighing around 2.5 kg were used in this study. All rabbits were provided by BioLASCO Taiwan Co, Ltd. (Taipei, Taiwan) and the Taipei Medical University Animal Care and Use Committee approved all the procedures. Animals were anesthetized with an intramuscular injection of 10 mg/kg zoletil for the study. A 10-mm filter paper soaked in 75% ethanol was applied on both the eyes of rabbits for 60 seconds, followed by a rinse of PBS. Then, 200 μL of *m*SC nanogel (200 μg/mL) was dropped in the left cornea and the right cornea received PBS buffer as a control. The injured eyes were stained with 1 mg/mL fluorescein to demarcate the wounded area. The healing process of corneal epithelium was evaluated by histopathologic analysis and calculation of the wounded area and tear sampling for MMP-9 activity at 0, 6, 24, 72, and 96 h after injury. A fluorescein sodium solution was used to evaluate the healing ratio of the corneal epithelium. The area of the corneal wound was quantified from photographs by using image analysis software (Power Image Analysis System Ching Hsing Computer-Tech Ltd, Taipei, Taiwan). The healing rate was expressed as the wounding area divided by the original wound area.

Histopathologic analysis

Rabbit corneas were harvested for histopathologic analysis on the scheduled time (6, 24, 48, 72, and 96 h). After fixation in formaldehyde (10%), the corneas were embedded in paraffin and the sectioned corneas were stained with hematoxylin-eosin for microscopic observation with light microscopy (Olympus BX51; Olympus, Tokyo, Japan) and photographed by digital camera (Olympus Digital Camera Camedia C-5050 Zoom).

MMP-9 activity

Tear samples were added to 10% zymogram gel. The gel was run at a constant 125 V at 30 mA. After 2 h, the gel was incubated in renaturing buffer (25% [v/v] Triton X-100 solution) for 0.5 h and then it was replaced with developing buffer. After 0.5 h at room temperature, the gel was placed on a rocker platform for overnight incubation. The developing buffer was replaced with Coomassie stain and the gel was incubated at room temperature on an orbital shaker for 20 min. The stain was replaced with destain buffer (30% methanol solution) and incubated for 10 min on an orbital shaker. Destain buffer was replaced with deionized water and the gel was photographed with a digital camera.

Statistical analysis

All the results were expressed as the mean ± standard deviation (SD). Data were compared between treatment groups using one-way Analysis of Variance (ANOVA). Differences were considered significant at $P < 0.05$.

Results and discussion

In traditional medicines, *Ganoderma tsugae* is used and has been proven to have various biological and pharmacological properties. The extracted residue of the *Ganoderma* fruiting body, named sacchachitin, also exhibits some biological activities. In an attempt to extend its potential application, we have assessed the suitability for corneal wound repair. The analytical result of the acid-treated hydrolyte from *m*SC using TLC and the dinitrosalicylic acid assay revealed that the main constituents of *m*SC are N-acetylglucosamine and glucose. These findings are consistent with our previous research on sacchachitin.

Microscopic examination of sacchachitin samples using scanning electron microscopy before and after milling clearly showed that the fibrous shape of mycelium (Figure 1A) was transformed into small particles or shorter fibers that were hydrated to form a gel matrix (Figure 1B). Although *m*SC was measured by particle size analyzer as having an average effective diameter of 2.06 μm with a mid-range polydispersity index (0.459), it was observed under SEM as having no sign of particles but appearing to be more like the gel matrix. This indicates not only that the average effective diameter of *m*SC measured should be designated as the fiber length but also that the diameter of those short fibers of *m*SC was so small in both length and diameter that they could be hydrated to become nanogel when *m*SC was dispersed in aqueous medium, as shown by Figure 1B. Further, the zeta potential of *m*SC was found to be as negative as −22.59 mV. This might indicate that the N-acetyl glucosamine unit in the structural skeleton of sacchachitin was not hydrolyzed to glucosamine as basic $-NH_2$ during preparation of *m*SC from the residue of the *Ganoderma* fruit body.

Since nanogel was formed when *m*SC was dispersed in the aqueous solution, we performed rheological analysis to investigate the structure and characteristics of *m*SC nanogel; the results are illustrated in Figure 2. Steady viscosities (η) of nanogels dispersed in deionized water as a function of shear rates at 25°C are shown in Figure 2A. The viscosities of nanogel dispersions decrease rapidly with an increase of shear rates. Similar to typical pseudoplastic fluids, this demonstrates shear thinning as a result of elongating the random coil of those *m*SC fibers interacting with water along the shear direction and breaking down of the network formed by *m*SC fiber-*m*SC fiber interaction. Figure 2B further demonstrates a dynamic stress sweep study performed on this sample from 0.2 to 20.0 Pa. Constant G′ and G″ values at the lower shear stress region were observed, while a rapid drop of both values at higher shear stress appeared with the extent of reduction being greater for G′ than that for G″. Since G′ was designated as elastic modulus and G″ as viscous modulus, it indicates that the network composed of the particle-like domain of *m*SC fiber-*m*SC fiber interaction is easier to be broken down than that of the viscous gel domain composed of hydrated *m*SC fibers. Figure 2B also shows changes of complex viscosities (η*) as a function of stresses for *m*SC nanogel at 25°C. The η* of *m*SC nanogel decreases with increasing stress after the gel structure of *m*SC breaks down, at which point the applied shear stress was higher than the yield stress. The result also reveals that *m*SC nanogel is a pseudoplastic flow with lower viscosities at 25°C.

Figure 2C illustrates a dynamic viscoelasticity test performed on the *m*SC nanogel. As shown, the storage modulus

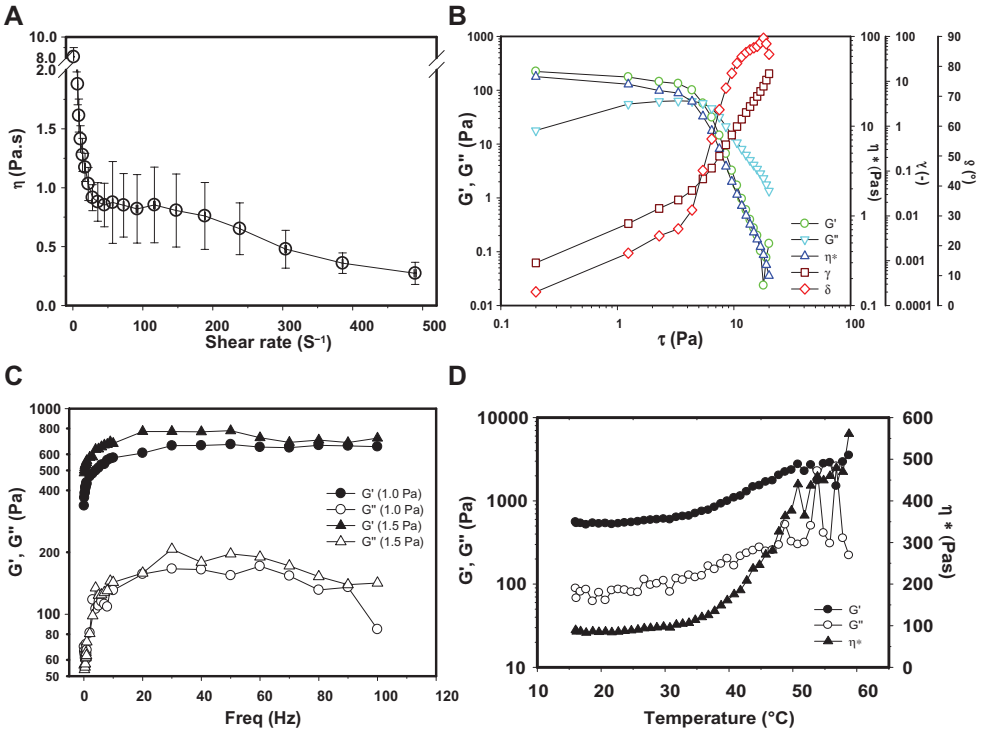

Figure 2 Rheological characteristics of aqueous solution of *m*SC nanogel (3% w/v) at 25 °C. (**A**) Viscosities as a function of shear rate; (**B**) Dynamic stress sweep study; (**C**) Frequency sweep curves; (**D**) Dynamic temperature ramp curves.
Abbreviations: *m*SC, micronized sacchachitin; SD, standard deviation.

(G′) and loss modulus (G″) of *m*SC nanogel as a function of frequency were obtained by a dynamic frequency sweep from 0.1 to 100 Hz at a constant stress of 1.0 and 1.5 Pa at 25°C. The relationship of G′ and G″, depending on frequency, usually reflects the interaction between *m*SC fibers and between *m*SC and the surrounding water. The G′ value is higher than the G″ value over the whole range of frequencies at these two stresses, indicating that *m*SC nanogel is predominantly elastically solid at room temperature. Both G′ and G″ increase rapidly in the initial period of the frequency increase, suggesting the strong frequency dependence of both modulus. Thereafter, both modules increase slowly as the frequency exceeds 10 Hz, which is likely a result of the formation of a transient 3D percolation network induced by the fast colliding rate of *m*SC fibers at high frequencies. Figure 2D shows the dynamic temperature ramp curves of *m*SC nanogel at a frequency of 1 Hz and a stress of 1 Pa. With an increase of temperature, the rheological parameters (G′, G″, and η*) first gradually increase in the temperature range of 20°C–35°C and then increase remarkably at the temperature around 37°C. The phenomena might be due to the hydrophilicity of *m*SC fibers, which leads to a strong interaction of *m*SC fiber-*m*SC fiber and *m*SC fiber-water via hydrogen bonding.

The direct biological consequence of *m*SC nanogel stimulation on SIRC cells was investigated using an MTT cell proliferation study and migration assay. As shown in Figure 3, SIRC cells in the *m*SC nanogel treatment group proliferated significantly at 24 and 48 h compared to those in the control group (PBS buffer only). At the concentration of 200, 300, and 400 μg/mL, *m*SC nanogel significantly increased SIRC cell proliferation after 24 h of incubation. The longer incubation time (48 h) and lesser concentration of 80, 100, and 200 μg/mL respectively of *m*SC nanogel also resulted in a significant amount of SIRC proliferation. When treated with 200 μg/mL of *m*SC nanogel, SIRC

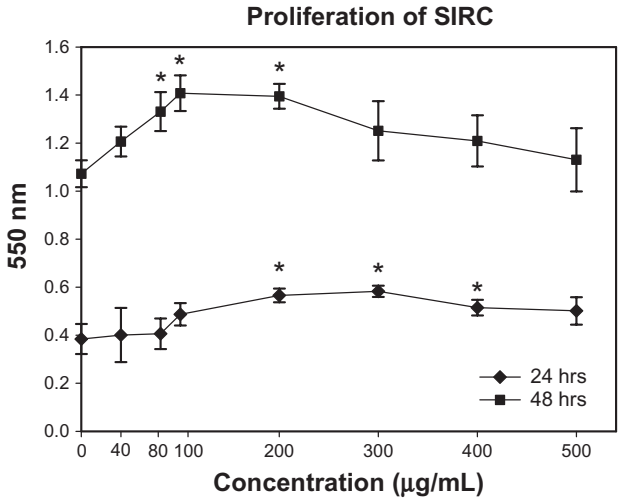

Figure 3 Results of the MTT cell proliferation assay (mean ± SD).
Note: Statens Seruminstitut rabbit cornea (SIRC) cells were treated with various concentrations of *m*SC for 24 and 48 h.
Abbreviations: *m*SC, micronized sacchachitin; MTT, 3-(4,5-Dimethylthiazol-2-yl)-2,5-diphenyltetrazolium bromid; SD, standard deviation.

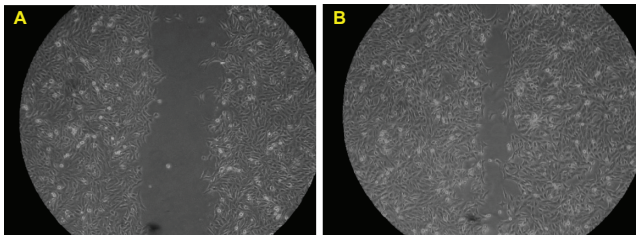

Figure 4 Representative phase contrast images of the migration assay to assess the effects of *m*SC suspension (200 μg/mL) in the media on wound closure. The images represent time-lapse images at time 0 (**A**) and 24 h later (**B**).
Abbreviation: *m*SC, micronized sacchachitin.

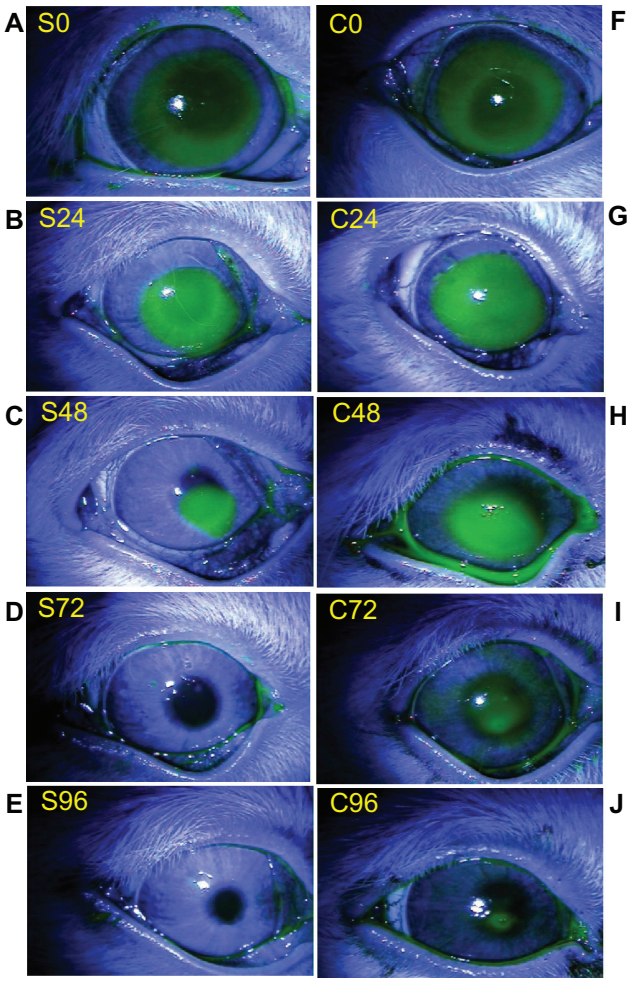

Figure 5 Fluorescein staining micrograph of a representative corneal wound obtained at 0, 24, 48, 72, and 96 h after wounding. The left column (**A–E**) represents corneas treated with *m*SC suspension (200 μg/mL), and the right column (**F–J**) represents corneas treated with phosphate-buffered saline.
Abbreviation: *m*SC, micronized sacchachitin.

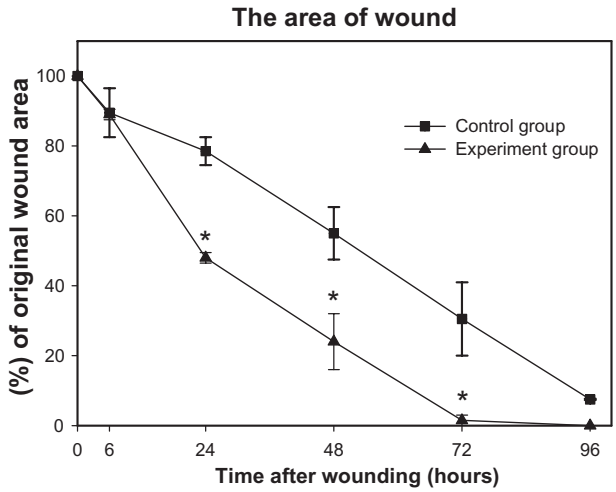

Figure 6 Percentage of rabbit corneal epithelial wound area in response to *m*SC treatment (Experimental group) compared to treatment with phosphate-buffered saline alone (Control group).
Note: *A paired *t*-test of significant difference with $P < 0.05$.
Abbreviation: *m*SC, micronized sacchachitin.

proliferated significantly in both incubation times (24 and 48 h, respectively), hence the concentration 200 µg/mL was chosen to being optimal for the following investigation. It is observed that the cell-proliferating effect was diminished when high-concentration *m*SC nanogel was applied (300 to 500 µg/mL). This may be explained by the toxicity and reinforcement of a low-affinity receptor, which alters the cellular response.[32] During wound healing, epithelial cells distal to the wound area are stimulated to migrate toward the wound for the restoration of corneal epithelial function. The migration assay has been previously employed as an in vitro model for epithelial cell migration during wound healing.[33] To examine the influence of the *m*SC nanogel on SIRC cells, further migration assay was applied, and results are shown in Figure 4. The evidence of cell migration was observed when the scratch in the cell monolayer gradually closed during incubation with 200 µg/mL *m*SC nanogel for 24 h.

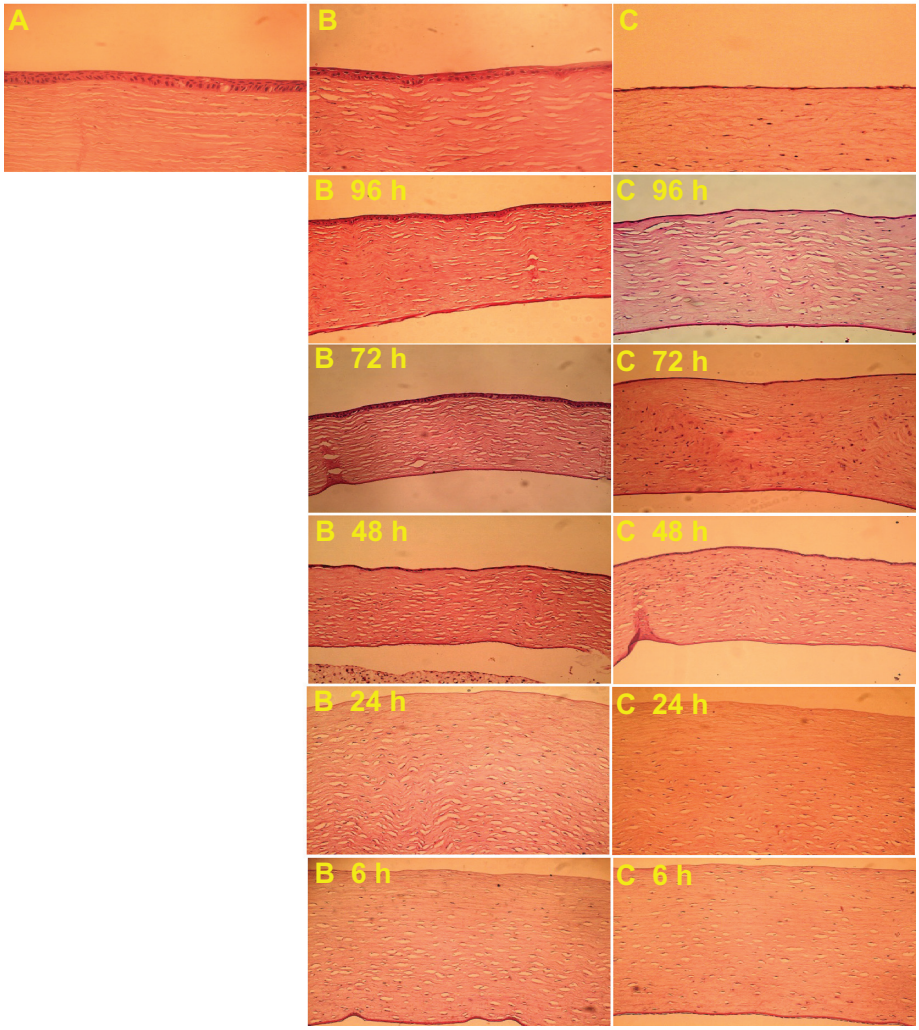

Figure 7 Histological examination of wounded rabbit corneas. (**A**) Normal cornea (**B**) mSC-treated group (**C**) Control group.
Abbreviation: *m*SC, micronized sacchachitin.

The integrity of corneal epithelium is important for maintaining the balance between epithelial and mesenchymal interactions, which play an active role in the chemokinetics of corneal wound healing. Diluted alcohol is frequently used for removal of the epithelium during photorefractive keratectomy (PRK) and laser subepithelial keratomileusis (LASEK).[10] Therefore, in this study we used alcohol for creating the corneal epithelial wound. To assess the corneal wound-healing effect of the *m*SC nanogel animal, a corneal wound model was used. Changes in the corneal wound area treated with *m*SC nanogel and PBS buffer separately were recorded at 6, 24, 48, 72, and 96 h post-wounding. Fluorescein staining indicated the location of the wound beds where the epithelial layers had been removed. The images representing the fluorescein staining wound area in rabbit corneas following treatment with PBS buffer and 200 μg/mL *m*SC nanogel are shown in Figure 5. No significant differences in wounded areas were observed between treatments during the first 24 h post-wounding. The healing with *m*SC nanogel treatment compared to the control group could be seen clearly at 72 h post-wounding. At 72 h post-wounding, complete wound closure was observed in the *m*SC nanogel-treated group; however, those of the control group still remained unhealed. The percentage of wounded area is shown in Figure 6. From 24 h post-wounding, the percentage of wounded area in the *m*SC nanogel-treated group was significantly smaller than that of the control group ($P < 0.05$).

Histological examination revealed that corneal epithelial cells appeared to form a layer covering all wounds treated with either PBS buffer or 200 μg/mL of *m*SC nanogel at 96 h post-wounding (Figure 7). The corneal epithelial cells appeared well stratified when compared to the normal corneal cells and the healing process was observed to be complete in the *m*SC nanogel-treated group. A relatively thinner layer of epithelial cells in the control group was seen when compared to those in the *m*SC nanogel-treated group along with infiltration of inflammatory cells, which appeared mildly inflamed in the wounded area. As was observed at 24 and 48 h, the result of analysis of the MMP-2 and MMP-9 activities from the tear samples (Figure 8) of the experimental group as compared to the control group displayed a significant decrease in MMP-9 activity, whereas only minor activity of MMP-2

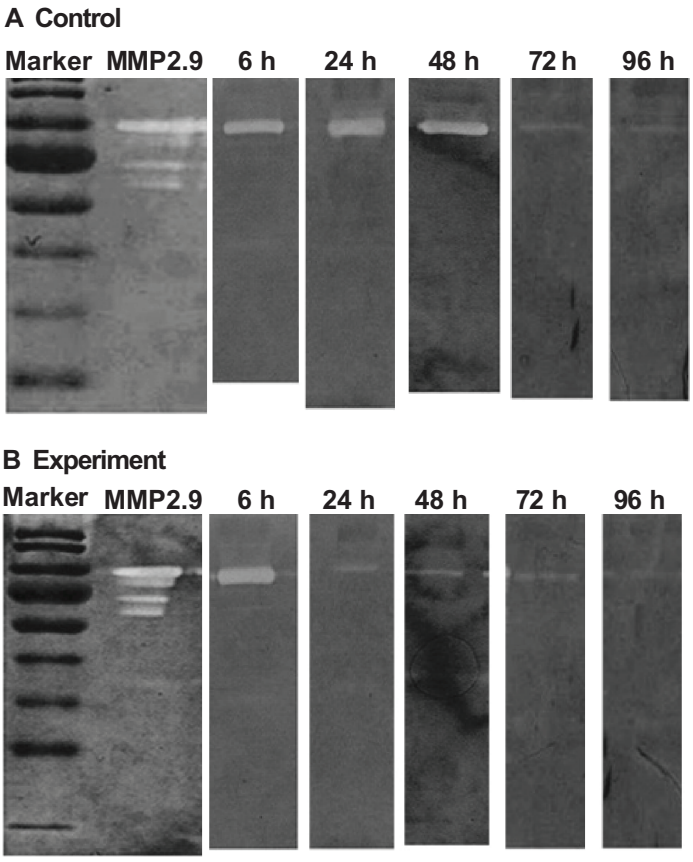

Figure 8 Variation in matrix metalloproteinase-9 (MMP-9) expression of the rabbit cornea at 6, 24, 48, 72, and 96 hours (h) during wound healing. SDS polyacrylamide gel electrophoretic analysis of tear samples from repairing cornea. Exp represents the experimental group (200 μg/mL *m*SC). Con represents the control group (phosphate-buffered saline). (**A**) MMP-9 expression of the experimental group (**B**) MMP-9 expression of the control group.

was observed. MMP-9, the matrix-degrading enzyme, is highly expressed at the site of inflammation and involved in remodeling processes. It also facilitates the recruitment of inflammatory cells such as eosinophils and neutrophils across basement membranes.[34] It is known that in damaged corneas, proteolysis in the tear fluid has been found to be significantly increased compared to normal eyes. In this study, the reduction of MMP-9 activity in the tear samples can be viewed as the healing of corneal wound. Based on our previous studies, sacchachitin can inhibit MMPs (MMP-1, MMP-8, and MMP-9) activity by its binding effect. The acceleration of corneal wound healing by *m*SC nanogel is probably due to the reduction in MMP-9 activity (not MMP-2) and attenuating the inflammation at the wound site.

Conclusions

Nanogel from micronized sacchachitin (*m*SC) was successfully produced and the chemical and physical properties were identified and confirmed as in a previous publication. Rheological characteristics were also studied for nanogel formed by dispersing *m*SC in aqueous solution. In vitro cell proliferation study and cell migration assay revealed a significant increase in SIRC cell proliferation and wound closure stimulation by *m*SC nanogel treatment. In an animal study, enhancement of corneal epithelial wound healing was observed, due to the inhibition of proteolytic activity. Concluding the findings, the study substantiates the potential application of sacchachitin as *m*SC nanogel for the treatment of superficial corneal injuries.

Acknowledgments

Financial support by the National Council of Science, ROC (NSC97-2320-B-038-005- MY3) and Department of Health, Executive Yuan, ROC (DOH101-TD-B-111-003) is highly appreciated.

Disclosure

The authors report no other conflicts of interest in this work.

References

1. Fish R, Davidson RS. Management of ocular thermal and chemical injuries, including amniotic membrane therapy. *Curr Opin Ophthalmol*. 2010;21:317–321.
2. Tuft SJ, Shortt AJ. Surgical rehabilitation following severe ocular burns. *Eye (Lond.)* 2009;23:1966–1971.
3. Tejwani S, Kolari RS, Sangwan VS, Rao GN. Role of amniotic membrane graft for ocular chemical and thermal injuries. *Cornea*. 2007;26:21–26.
4. Tseng SC, Prabhasawat P, Barton K, et al. Amniotic membrane transplantation with or without limbal allografts for corneal surface reconstruction in patients with limbal stem cell deficiency. *Arch Ophthalmol*. 1998;116:431–441.
5. Meller D, Pires RTF, Mack RJS, Figueiredo F, et al. Amniotic membrane transplantation for acute chemical or thermal burns. *Ophthalmology*. 2000;107:980–990.
6. Wilson SE, Mohan RR, Mohan RR, Ambrosio R, Hong JW, Lee JS. The corneal wound healing response: cytokine-mediated interaction of the epithelium, stroma, and inflammatory cells. *Prog Retinal Eye Res*. 2001;20:625–637.
7. Steele C. Corneal wound healing: a review. *Optometry Today*. 1999;24: 28–32.
8. Kuo IC. Corneal wound healing. *Curr Opin Ophthalmol*. 2004;15: 311–315.
9. Robert AR. Tetracyclines and the treatment of corneal stromal ulceration: a review. *Cornea*. 2000;19:274–277.
10. Fini ME, Cook JR, Mohan R. Proteolytic mechanisms in corneal ulceration and repair. *Arch Dermatol Res*. 1998;290 Suppl: S12–S23.
11. Toriseva M, Kahari VM. Proteinases in cutaneous wound healing. *Cell Mol Life Sci*. 2009;66:203–224.
12. Mulholland B, Tuft SJ, Khaw PT. Matrix metalloproteinase distribution during early corneal wound healing. *Eye*. 2005;19:584–588.
13. Ollivier FJ, Gilger BC, Barrie KP, et al. Proteinases of the cornea and preocular tear film. *Vet Ophthalmol*. 2007;10:199–206.
14. Predović J, Balog T, Marotti T, et al. The expression of human corneal MMP-2, MMP-9, proMMP-13 and TIMP-1 in bullous keratopathy and keratoconus. *Coll Antropol*. 2008;32(Suppl 2):15–19.
15. Mohan R, Chintala SK, Jung JC, et al. Matrix metalloproteinase gelatinase B (MMP-9) coordinates and effects epithelial regeneration. *J Biol Chem*. 2002;277:2065–2072.
16. Barro CD, Romanet JP, Fdili A, Guillot M, Morel F. Gelatinase concentration in tears of corneal-grafted patients. *Curr Eye Res*. 1998;17: 174–182.
17. Kim JS, Kim JC, Na BK, Jeong JM, Song CY. Amniotic membrane patching promotes healing and inhibits proteinase activity on wound healing following acute corneal alkali burn. *Exp Eye Res*. 2000;70: 329–337.
18. Anderson SB, de Souza RF, Hofmann-Rummelt C, Seitz B. Corneal calcification after amniotic membrane transplantation. *Br J Ophthalmol*. 2003;87:587–591.
19. Shahriari HA, Tokhmehchi F, Mohammad R, Hashemi NF. Comparison of the effect of amniotic membrane suspension and autologous serum on alkaline corneal epithelial wound healing in the rabbit model. *Cornea*. 2008;27:1148–1150.
20. Willoughby CE, Batterbury M, Kaye SB. Collagen corneal shields. *Surv Ophthalmol*. 2002;47:174–182.
21. Hori K, Sotozono C, Hamuro J, et al. Controlled-release of epidermal growth factor from cationized gelatin hydrogel enhances corneal epithelial wound healing. *J Control Release*. 2007;118:169–176.
22. Márquez-de-Aracena R, Montero-de-Espinosa I, Muñoz M, Pereira G. Subconjunctival application of plasma platelet concentrate in the treatment of ocular burns. Preliminary results. *Arch Soc Esp Oftalmol*. 2007; 82(8):475–481.
23. Márquez-de-Aracena R, Montero-de-Espinosa I. Subconjunctival application of regenerative factor-rich plasma for the treatment of ocular alkali burns. *Eur J Ophthalmol*. 2009;19(6):909–915.
24. Garrett Q, Xu S, Simmons PA, et al. Carboxymethyl cellulose stimulates rabbit corneal epithelial wound healing. *Curr Eye Res*. 2008;33: 567–573.
25. Jang IK, Ahn JI, Shin JS, et al. Transplantation of reconstructed corneal layer composed of corneal epithelium and fibroblasts on a lyophilized amniotic membrane to severely alkali-burned cornea. *Artif Organs*. 2006;30:424–431.
26. Pratoomsoot C, Tanioka H, Hori K, et al. A thermoreversible hydrogel as a biosynthetic bandage for corneal wound repair. *Biomaterials*. 2008;29:272–281.
27. Gordon MK, Desantis A, Deshmukh M, et al. Doxycycline hydrogels as a potential therapy for ocular vesicant injury. *J Ocul Pharmacol Ther*. 2010;26:407–419.

28. Du LQ, Wu XY, Li MC, Wang SG, Pang KP. Effect of different biomedical membranes on alkali-burned cornea. *Ophthalmic Res*. 2008;40:282–290.
29. Su CH, Sun CS, Juan SW, Hu CH, Ke WT, Sheu MT. Fungal mycelia as the source of chitin and polysaccharides and their applications as skin substitutes. *Biomaterials*. 1997;18:1169–1174.
30. Su CH, Sun CS, Juan SW, Ho HO, Hu CH, Sheu MT. Development of fungal mycelia as skin substitutes: effects on wound healing and fibroblast. *Biomaterials*. 1999;20:61–68.
31. Su CH, Liu SH, Yu SY, et al. Development of fungal mycelia as a skin substitute: characterization of keratinocyte proliferation and matrix metalloproteinase expression during improvement in the wound-healing process. *J Biomed Mater Res A*. 2005;72:220–227.
32. Chan BP, Chan KM, Maffulli N, Webb S, Lee KH. Effect of basic fibroblast growth factor: an *in vitro* study of tendon healing. *Clin Orthop Relat Res*. 1997;342:239–247.
33. Pellegrini G, Golisano O, Paterna P, Lambiase A, Bonini S, Rama P. Location and clonal analysis of stem cells and their differentiated progeny in the human ocular surface. *J Cell Biol*. 1999;145:769–782.
34. Lee YC, Lee HB, Rhee YK, Song CH. The involvement of matrix metalloproteinase-9 in airway inflammation of patients with acute asthma. *Clin Exp Allergy*. 2001;31:1623–1630.